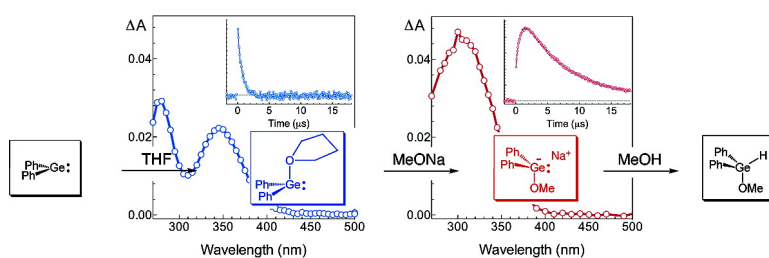


Fast Kinetic Studies of the Reactivities of Transient Germlyenes in Methanol and Tetrahydrofuran Solution

Farahnaz Lollmahomed, Lawrence A. Huck, Cameron R. Harrington, Saurabh S. Chitnis, and William J. Leigh

Organometallics, 2009, 28 (5), 1484-1494 • Publication Date (Web): 09 February 2009

Downloaded from <http://pubs.acs.org> on March 2, 2009



More About This Article

Additional resources and features associated with this article are available within the HTML version:

- Supporting Information
- Access to high resolution figures
- Links to articles and content related to this article
- Copyright permission to reproduce figures and/or text from this article

[View the Full Text HTML](#)

Fast Kinetic Studies of the Reactivities of Transient Germynes in Methanol and Tetrahydrofuran Solution

Farahnaz Lollmahomed, Lawrence A. Huck, Cameron R. Harrington, Saurabh S. Chitnis, and William J. Leigh*

Department of Chemistry, McMaster University, 1280 Main Street West, Hamilton, Ontario, Canada L8S 4M1

Received October 27, 2008

Laser flash photolysis techniques have been employed to study the reactivities of dimethylgermylene (GeMe_2), diphenylgermylene (GePh_2), and a series of ring-substituted diarylgermylenes (GeAr_2) in methanol (MeOH) and tetrahydrofuran (THF) solution, where the germynes exist as the corresponding Lewis acid–base complexes with the O-donor solvents. Dimerization to the corresponding digermene is a significant mode of decay in THF solution, particularly for the GeMe_2 –THF complex, though for the diaryl systems it is slowed dramatically compared to the situation in hexane solution. On the other hand, dimerization is undetectable in MeOH, where the GeAr_2 –MeOH complexes decay with pseudo-first-order kinetics at low laser intensities and lifetimes in the 20–50 μs range; the GeMe_2 –MeOH complex exhibits a lifetime of ca. 4 μs under similar conditions. Solvent kinetic isotope effects are consistent with solvent-catalyzed proton transfer to yield the corresponding alkoxyhydridogermene as the process responsible for the decay of the germylene–MeOH complexes. Their decay is accelerated by strong acids and bases such as methanesulfonic acid and sodium methoxide, respectively, which quench the GePh_2 –MeOH complex with rate constants of ca. $3 \times 10^9 \text{ M}^{-1} \text{ s}^{-1}$ in each case. Kinetic isotope and substituent effects are consistent with rate-determining protonation at germanium in the reactions with acid, while the results for methoxide quenching are consistent with the formation of the corresponding $\text{Ar}_2(\text{MeO})\text{Ge}^-$ anion as a discrete intermediate, which has been detected in MeOH solution in one instance. Reaction of sodium methoxide with the germylene–THF complexes also proceeds rapidly and allows the detection of the corresponding $\text{Ar}_2(\text{MeO})\text{Ge}^-$ anions and determination of rate coefficients for their protonation by MeOH, for all four of the diaryl systems that were studied. The reactivity of the GeMe_2 –THF complex toward sodium methoxide, methanesulfonic and acetic acid, CCl_4 , oxygen, isoprene, and 4,4-dimethyl-1-pentene has also been examined.

Introduction

The chemistry of silylenes and germynes, the silicon and germanium analogues of carbenes, has received considerable attention over the past few decades.^{1–9} One aspect of their reactivities that has been of particular interest is Lewis acid–base complexation with O- and N-donors, a process that can mediate the rates and selectivities of their reactions^{10–18} and is known to be the initial step in the well-known O–H and

N–H insertion reactions of these species with alcohols^{11,19–24} and primary or secondary amines.^{20,22,25–27} Complexes of transient silylenes and germynes with ethers, amines, and other donors have been detected spectroscopically both in low-temperature matrixes^{12,21,28–30} and in solution.^{11,24,31,32} The reactions of the parent species (SiH_2 and GeH_2) with water,

* Corresponding author. E-mail: leigh@mcmaster.ca.

(1) Gaspar, P. P.; Jones, M., Jr.; Moss, R. A. In *Reactive Intermediates*; John Wiley & Sons: New York, 1978; Vol. 1, pp 229–277.

(2) Neumann, W. P. *Chem. Rev.* **1991**, *91*, 311.

(3) Driess, M.; Grützmacher, H. *Angew. Chem., Int. Ed. Engl.* **1996**, *35*, 828.

(4) Gaspar, P. P.; West, R.; Rappoport, Z.; Apeloig, Y. In *The Chemistry of Organic Silicon Compounds*; Rappoport, Z., Ed.; John Wiley and Sons: New York, 1998; Vol. 2, pp 2463–2568.

(5) Tokitoh, N.; Okazaki, R. *Coord. Chem. Rev.* **2000**, *210*, 251.

(6) Kira, M.; Ishida, S.; Iwamoto, T. *Chem. Rec.* **2004**, *4*, 243.

(7) Tokitoh, N.; Ando, W.; Moss, R. A.; Platz, M. S.; Jones, M., Jr. In *Reactive Intermediate Chemistry*; John Wiley & Sons: New York, 2004; pp 651–715.

(8) Boganov, S. E.; Egorov, M. P.; Faustov, V. I.; Krylova, I. V.; Nefedov, O. M.; Becerra, R.; Walsh, R. *Russ. Chem. Bull. Int. Ed.* **2005**, *54*, 483.

(9) Becerra, R.; Walsh, R. *Phys. Chem. Chem. Phys.* **2007**, *9*, 2817.

(10) Steele, K. P.; Weber, W. P. *J. Am. Chem. Soc.* **1980**, *102*, 6095.

(11) Levin, G.; Das, P. K.; Bilgrien, C.; Lee, C. L. *Organometallics* **1989**, *8*, 1206.

(12) Belzner, J.; Ihmels, H. *Adv. Organomet. Chem.* **1999**, *43*, 1.

(13) Sanji, T.; Mitsugi, H.; Tanaka, M.; Fujiyama, H.; Sakurai, H. *Organometallics* **2006**, *25*, 6159.

(14) Rivière, P.; Satgé, J.; Castel, A. C. R. *Acad. Sci. Paris* **1975**, *281*, 835.

(15) Egorov, M. P.; Dvornikov, A. S.; Ezhova, M. B.; Kuz'min, V. A.; Kolesnikov, S. P.; Nefedov, O. M. *Organomet. Chem. USSR* **1991**, *4*, 582.

(16) Wienken, S.; Neumann, W. P. *Chem. Ber.* **1993**, *126*, 769.

(17) Schoeller, W. W.; Schneider, R. *Chem. Ber.* **1997**, *130*, 1013.

(18) Bonnefille, E.; Mazières, S.; Hawi, N. E.; Gornitzka, H.; Couret, C. *J. Organomet. Chem.* **2006**, *691*, 5619.

(19) Steele, K. P.; Weber, W. P. *Inorg. Chem.* **1981**, *20*, 1302.

(20) Raghavachari, K.; Chandrasekhar, J.; Gordon, M. S.; Dykema, K. J. *J. Am. Chem. Soc.* **1984**, *106*, 5853.

(21) Gillette, G. R.; Noren, G. H.; West, R. *Organometallics* **1989**, *8*, 487.

(22) Su, M. D.; Chu, S. Y. *J. Phys. Chem. A* **1999**, *103*, 11011.

(23) Heaven, M. W.; Metha, G. F.; Buntine, M. A. *J. Phys. Chem. A* **2001**, *105*, 1185.

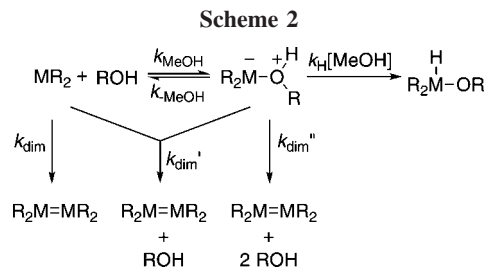
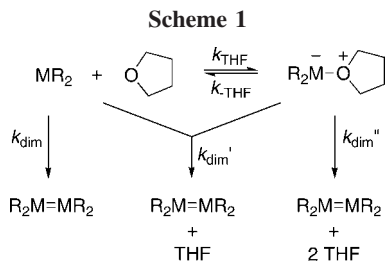
(24) Leigh, W. J.; Lollmahomed, F.; Harrington, C. R.; McDonald, J. M. *Organometallics* **2006**, *25*, 5424.

(25) Becerra, R.; Cannady, J. P.; Walsh, R. *Silicon Chem.* **2005**, *3*, 131.

(26) Leigh, W. J.; Harrington, C. R. *J. Am. Chem. Soc.* **2005**, *127*, 5084.

(27) Huck, L. A.; Leigh, W. J. *Organometallics* **2007**, *26*, 1339.

(28) Gillette, G. R.; Noren, G. H.; West, R. *Organometallics* **1987**, *6*, 2617.



methanol, and dimethyl ether in the gas phase have been characterized by fast kinetic methods^{33–35} and have also been the subject of numerous theoretical studies.^{17,20,23,36–42}

The results of recent fast kinetic studies of the reactions of the homologous silylenes and germynes MR_2 ($M = Si$ or Ge ; $R = Me$ or Ph) with tetrahydrofuran (THF) in hexane solution^{24,32} provide a useful starting point for comparing the kinetics and thermodynamics of Lewis acid–base complexation for the two types of species. The results can be considered within the common mechanistic framework of Scheme 1, which depicts the complexation process as a reversible reaction occurring in competition with formation of the corresponding dimetallene dimer, M_2R_4 . The following trends emerge from the data.

Complexation with THF in hexane solution proceeds at or close to the diffusion-controlled limit in all cases, but is marginally slower for the germynes. Similarly, the UV/vis absorption maxima of the MR_2 –THF complexes are markedly blue-shifted relative to those of the free metallylene, but there is little to no detectable difference in λ_{max} for the silylene– and germylene–THF complexes of otherwise identical substitution; thus, $\lambda_{max} \approx 355$ nm for the THF complexes of $SiPh_2$ and $GePh_2$, and $\lambda_{max} \approx 310$ nm for those of $SiMe_2$ and $GeMe_2$.^{24,32} In spite of these similarities, the process is substantially more favorable thermodynamically for the silylene than for the germylene of otherwise identical substitution. Complexation with the germynes exhibits the distinctive signs of reversibility at millimolar THF concentrations, the data permitting determination of equilibrium constants of $K_{THF} \approx 23\,000\ M^{-1}$ and $K_{THF} \approx 10\,000\ M^{-1}$ for complexation with $GePh_2$ and $GeMe_2$, respectively, where $K_{THF} = k_{THF}/k_{-THF}$.²⁴ In contrast, the kinetic behavior exhibited by the silylenes is consistent with equilibrium constants for complexation in excess of $10^5\ M^{-1}$ under similar conditions.³² Dimerization, which proceeds at close to the diffusion-controlled rate for the free metallylenes, is slower but is not eliminated in the presence of THF; $k_{dim} > k_{dim}' > k_{dim}''$.^{24,32}

The kinetic characteristics of the reactions of methanol with the dimethyl- and diphenylmetallylenes (Scheme 2) show a number of similarities to those for THF complexation.^{24,43} For example, the rate-determining step for metallylene consumption is formation of the intermediate complex for all species, the rate constants for which are again very close to the diffusional limit for the silylenes⁴³ and only modestly slower for the germynes.²⁴ Equilibrium constants cannot be measured for the silylenes, but those for complexation of the germynes with MeOH are 6–10 times smaller than those for complexation of the same species with THF. They nevertheless follow the same trend with substituent, with the faster-reacting germylene ($GeMe_2$) forming the thermodynamically less stable complex: $K_{MeOH} = 3300\ M^{-1}$ for $GePh_2$ and $900\ M^{-1}$ for $GeMe_2$.²⁴ The most pronounced differences between the silylenes and the germynes are associated with the kinetic behavior of the corresponding complexes. Short-lived transient absorptions in the same spectral ranges as those due to the corresponding THF complexes can be observed for both $SiMe_2$ and $SiPh_2$ in the presence of submillimolar concentrations of MeOH, but vanish at higher alcohol concentrations. This is consistent with a rapid catalytic route involving a second molecule of alcohol for the product-forming H-migration process; as would be expected, disilene formation is quenched efficiently in the presence of submillimolar concentrations of MeOH.⁴³ The GeR_2 –MeOH complexes also exhibit similar absorption spectra to those of the corresponding THF complexes, but are remarkably long-lived, decaying with complex kinetics over several tens of microseconds, coincident with the growth of the corresponding digermenes. Thus, the catalytic proton transfer process required to convert the complex to the final (alkoxymetallane) product is many orders of magnitude slower for the germynes than for the silylenes, indicating a quite remarkable difference in the acid–base characteristics of silylene–alcohol and germylene–alcohol complexes.

In the present paper, we report the results of a laser flash photolysis study of the chemistry of the MeOH and THF complexes of $GeMe_2$, $GePh_2$, and a series of substituted diarylgermylenes ($GeAr_2$: $Ar = 4-MeC_6H_4$; $3,4-Me_2C_6H_3$; $4-FC_6H_4$; $4-(CF_3)C_6H_4$) in the respective (neat) O-donors as solvents, employing the 1-germacyclopent-3-ene derivatives **1a–e** and **3** as photochemical precursors of the corresponding diarylgermylenes **2a–e**^{27,44} and $GeMe_2$,^{24,45} respectively (eqs 1 and 2). The study focuses mainly on their reactivities toward Brønsted acids (methanesulfonic and acetic acid) and sodium methoxide, exploring the role of acid–base catalysis in the formal O–H insertion reaction with alcohols and the reactivities of germylene–ether complexes toward protonation and nucleophilic substitution. The reaction with methoxide ion affords the

(29) Ando, W.; Itoh, H.; Tsumuraya, T.; Yoshida, H. *Organometallics* **1988**, *7*, 1880.

(30) Ando, W.; Itoh, H.; Tsumuraya, T. *Organometallics* **1989**, *8*, 2759.

(31) Yamaji, M.; Hamanishi, K.; Takahashi, T.; Shizuka, H. *J. Photochem. Photobiol. A: Chem.* **1994**, *81*, 1.

(32) Moiseev, A. G.; Leigh, W. J. *Organometallics* **2007**, *26*, 6277.

(33) Alexander, U. N.; King, K. D.; Lawrance, W. D. *Phys. Chem. Chem. Phys.* **2001**, *3*, 3085.

(34) Alexander, U. N.; King, K. D.; Lawrance, W. D. *J. Phys. Chem. A* **2002**, *106*, 973.

(35) Alexander, U. N.; King, K. D.; Lawrance, W. D. *Phys. Chem. Chem. Phys.* **2003**, *5*, 1557.

(36) Conlin, R. T.; Laakso, D.; Marshall, P. *Organometallics* **1994**, *13*, 838.

(37) Nowek, A.; Leszczynski, J. *J. Phys. Chem. A* **1997**, *101*, 3784.

(38) Heaven, M. W.; Metha, G. F.; Buntine, M. A. *Aust. J. Chem.* **2001**, *54*, 185.

(39) Bharatam, P. V.; Moudgil, R.; Kaur, D. *Organometallics* **2002**, *21*, 3683.

(40) Boganov, S. E.; Faustov, V. I.; Egorov, M. P.; Nefedov, O. M. *Russ. Chem. Bull. Int. Ed.* **2004**, *53*, 960.

(41) Su, M. D. *Chem.–Eur. J.* **2004**, *10*, 6073.

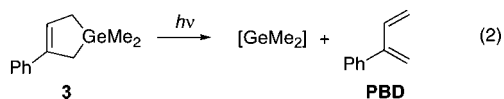
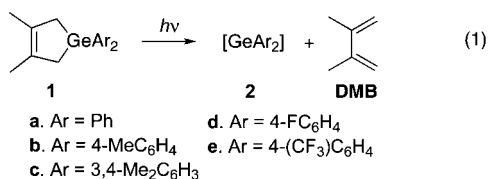
(42) Oláh, J.; De Proft, F.; Veszprémi, T.; Geerlings, P. *J. Phys. Chem. A* **2005**, *109*, 1608.

(43) Moiseev, A. G.; Leigh, W. J. *Organometallics* **2007**, *26*, 6268.

(44) Leigh, W. J.; Harrington, C. R.; Vargas-Baca, I. *J. Am. Chem. Soc.* **2004**, *126*, 16105.

(45) Leigh, W. J.; Lollmahomed, F.; Harrington, C. R. *Organometallics* **2006**, *25*, 2055.

corresponding $R_2(\text{MeO})\text{Ge}^-$ anions, which have been detected directly and their protonation kinetics determined for each of the aryl systems in THF and for one of them in MeOH. Finally, the reactivity of the GeMe_2 -THF complex toward an aliphatic diene, an alkene, oxygen, and carbon tetrachloride has also been examined.



Results and Discussion

Germacyclopentene **1c**, the only new germylene precursor examined in this work, was prepared by an analogous method to that employed for the other derivatives.^{27,44} Photolysis of the compound in C_6D_{12} containing MeOH (0.2 M) or isoprene (2 mM) led to the formation of 2,3-dimethyl-1,3-butadiene (DMB) and the expected trapping products of germylene **2c** by the added substrate in both cases. A value of $\Phi = 0.35 \pm 0.08$ was determined for the quantum yield of germylene extrusion from the compound, which is similar to but slightly lower than those reported earlier for the other compounds in the series.^{27,44} Complete details of the synthesis, characterization, and photochemical product studies of **1c** are provided in the Supporting Information.

Steady state photolysis (254 nm) of a deoxygenated solution of **1a** (0.045 M) in MeOH afforded diphenylmethoxygermane (**4a**) and 1,1,3,3-tetraphenyldigermoxane (**5**) as the major germanium-containing products, according to ^1H NMR analysis of the (evaporated) crude reaction mixture after ca. 50% conversion of **1a** (eq 3). The digermoxane was identified in the crude mixture by ^1H NMR and infrared spectroscopy⁴⁶ and is the expected product either of hydrolysis of **4a** during workup and/or of reaction of GePh_2 with adventitious water during the photolysis; its yield relative to **4a** was reduced significantly when the experiment was repeated using sodium-distilled MeOH. Similarly, photolysis of a deoxygenated solution of **3** (0.025 M) in THF- d_8 containing acetic acid (AcOH; 0.04 M) afforded acetoxydimethylgermane (**6**) (88%) and 2-phenyl-1,3-butadiene (PBD) (99%) as the only products detectable in the ^1H NMR spectrum of the crude reaction mixture after ca. 40% conversion of **3** (eq 4). The identification of **4a** and **6** as the major germanium-containing products in these experiments demonstrates (*inter alia*) that the major primary products of photolysis of **1a** and **3** in MeOH and THF solution (i.e., the corresponding germynes GePh_2 and GeMe_2 , respectively) and their trapping products are the same as they are in hexane under conditions of low light intensity.^{44,45}

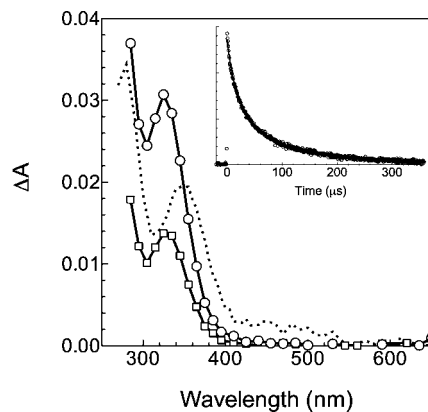
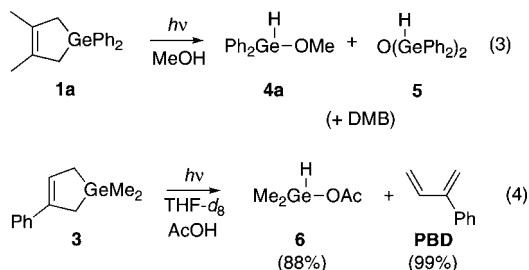
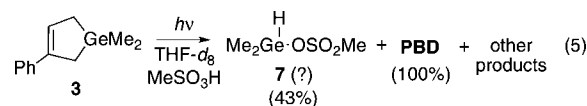


Figure 1. Transient absorption spectra from laser flash photolysis of **1a** in deoxygenated MeOH solution, recorded 0.19–0.83 μs (○) and 24.70–25.34 μs (□) after the laser pulse; the inset shows a transient decay trace recorded at 325 nm. The dotted line shows the spectrum obtained from the same compound in hexane containing 5 mM MeOH, recorded 90–116 ns after the pulse.

One additional steady state experiment was carried out, in which **3** was irradiated in THF- d_8 containing MeSO_3H (0.09 M) and monitored over time by ^1H NMR spectroscopy. The photolysis afforded PBD in quantitative yield and a number of additional products, one of which exhibited resonances at δ 5.90 (sept, 1H) and 0.76 (d, 6H). These features are the ones expected for germyl sulfonate ester **7** (eq 5), based on a comparison to the spectrum of **6** in the experiment described above (δ 5.60 (sept, 1H) and 0.56 (d, 6H)). The compound was formed in ca. 43% yield relative to consumed **3** and appeared to be sensitive to secondary photolysis. The other products formed in the reaction could not be identified.



Germylene–MeOH Complexes in MeOH. Laser photolysis of deoxygenated MeOH solutions of **1a–e** (ca. 0.003 M) afforded long-lived transient absorptions centered in the 320–330 nm range, on the edge of a more intense absorption centered below 280 nm. For example, Figure 1 shows transient spectra recorded by laser photolysis of **1a** in deoxygenated MeOH, along with a representative transient decay profile recorded at the absorption maximum of 325 nm. The species decays with mixed first- and second-order kinetics at normal laser intensities, but with clean pseudo-first-order kinetics and a lifetime of $\tau = 50 \pm 10 \mu\text{s}$ when the laser intensity is reduced using neutral density filters; in all five cases, the decay kinetics were the same throughout the 270–340 nm monitoring wavelength range, indicating that the spectra are due to a single transient species in each case. We assign the species to the corresponding GeAr_2 -MeOH complexes **8a–e**. The pseudo-first-order process that is responsible for their decay is assigned to solvent-catalyzed proton transfer, yielding the corresponding alkoxygermanes **4a–e** (eq 6). The spectra of the complexes are blue-shifted ca. 30 nm relative to those in dilute methanolic hexane, as illustrated in Figure 1 for **8a**.²⁴ The spectral shift may be the result of the much stronger solvation of the complex by hydrogen bonding that is possible in the neat alcohol relative to that in dilute hexane, though the possibility that it reflects a change in the preferred speciation of the complexes, from monocoordinate in dilute hexane to dicoordinate in the neat liquid, is difficult to rule out.

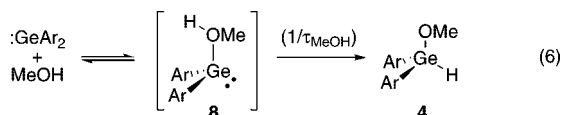
Table 1 lists the positions of the transient UV absorption maxima observed for **8a–e** in MeOH solution, along with

Table 1. UV Absorption Maxima, Pseudo-First-Order Decay Coefficients, and Absolute Rate Constants for Quenching of $\text{GeR}_2\text{-MeOH}$ Complexes (**8a–e**, **9**) by MeONa and MeSO_3H in MeOH at 25°C^a

R	λ_{max} (nm)	k_{MeOH}^b (10^4 s^{-1})	k_{MeONa}^b ($10^9 \text{ M}^{-1} \text{ s}^{-1}$)	$k_{\text{MeSO}_3\text{H}}^b$ ($10^9 \text{ M}^{-1} \text{ s}^{-1}$)
Ph (8a)	325	2.1 ± 0.6	3.03 ± 0.06	3.9 ± 0.2
4-(CH_3) C_6H_4 (8b)	325	2.5 ± 0.2	2.6 ± 0.2	4.3 ± 0.4
3,4-(CH_3) C_6H_3 (8c)	325	5.1 ± 1.4	1.9 ± 0.4	4.5 ± 0.5
4-(F) C_6H_5 (8d)	320	2.6 ± 1.0	4.0 ± 0.3	2.04 ± 0.07
4-(CF_3) C_6H_4 (8e)	330 (sh)	3.9 ± 1.6	3.7 ± 0.5^c	0.67 ± 0.03
Me (9)	≤ 295	25.7 ± 0.7	1.8 ± 0.2	7.7 ± 0.9

^a Errors reported as twice the standard error from least-squares analysis. ^b Average of four determinations of k_{decay} at low laser intensity. ^c Defined by k_{decay} at the lowest $[\text{MeONa}]$ value studied (see text).

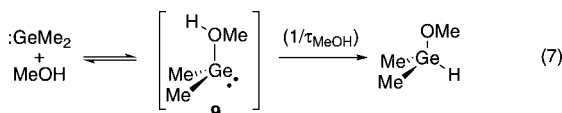
estimates of the pseudo-first-order rate coefficients for their decay (k_{MeOH} ; obtained at low laser intensities); the actual spectra obtained for these compounds are included in the Supporting Information (Figure S6).



- a. Ar = Ph
 b. Ar = 4-Me C_6H_4
 c. Ar = 3,4-Me $_2\text{C}_6\text{H}_3$
 d. Ar = 4-F C_6H_4
 e. Ar = 4-(CF_3) C_6H_4

An essentially identical transient spectrum to that shown in Figure 1 was obtained by laser photolysis of **1a** in deoxygenated MeOD solution. Again, the species decayed with mixed-order kinetics over a similar time scale to that observed in the protiated solvent under normal conditions, but with clean pseudo-first-order kinetics and $\tau = 120 \pm 30 \mu\text{s}$ at reduced laser intensities. Comparison of the latter to the first-order decay rate constant in MeOH yields a solvent isotope effect of $k_{\text{H}}/k_{\text{D}} = 2.5 \pm 0.8$, which is consistent with the conclusion above that solvent-catalyzed proton transfer comprises the rate-determining step for decay of the complex.

Laser photolysis of the GeMe_2 precursor **3** in deoxygenated MeOH also afforded a single transient absorption, assignable to the $\text{GeMe}_2\text{-MeOH}$ complex (**9**; eq 7), which decayed with clean first-order kinetics ($\tau \approx 4 \mu\text{s}$) and exhibited an apparent maximum at 295 nm, on the long-wavelength edge of the bleaching signal due to the precursor. The spectrum and a representative decay profile are shown in Figure 2, along with the previously reported spectrum obtained from the same compound in hexane containing 0.05 M MeOH.²⁴ The spectrum in neat MeOH shows little evidence of the blue shift relative to that in dilute hexane that is exhibited by the $\text{GeAr}_2\text{-MeOH}$ complexes, but this may be due to the fact that the absorptions due to **9** are on the edge of the precursor spectrum in both solvents, and thus the measured spectra are unlikely to be representative of the true transient absorption spectra under either set of conditions. It should be noted that **9** is ca. 10 times shorter-lived than **8a** under similar conditions, consistent with significantly faster pseudo-first-order decay of the less sterically hindered dialkylgermylene complex via solvent-catalyzed proton transfer, compared to the diphenyl system.



Addition of MeSO_3H to the MeOH solutions of **1a–e** and **3** caused enhancements in the decay rates of the absorptions

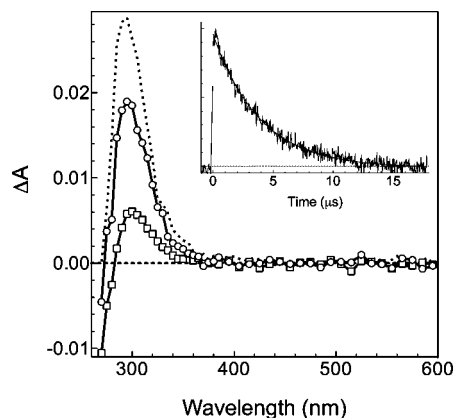


Figure 2. Transient absorption spectra from laser flash photolysis of **3** in deoxygenated MeOH, recorded 0.19–0.32 μs (–○–) and 4.51–4.74 μs (–□–) after the laser pulse; the inset shows a transient decay trace recorded at 300 nm. The dotted line shows the spectrum obtained for the same compound in hexane containing 0.05 M MeOH, recorded 260–290 ns after the pulse.

due to the germylene–MeOH complexes and a change to clean pseudo-first-order kinetics. Plots of the pseudo-first-order decay rate constants (k_{decay}) vs $[\text{MeSO}_3\text{H}]$ were linear over the concentration ranges studied in all six cases (0.1–1.1 mM with **1a–d** and **3**; 1.5–15.5 mM with **1e**) and were thus analyzed according to eq 8, where k_0 is the pseudo-first-order rate constant for decay of the germylene–solvent complex in the absence of added substrate (i.e., k_{MeOH} in Table 1), and k_Q is the bimolecular rate constant for quenching of the complex by the substrate, Q. Figure 3a shows the plots for quenching of **8a–e** by MeSO_3H , while the associated k_Q values ($k_{\text{MeSO}_3\text{H}}$) are listed in Table 1.

$$k_{\text{decay}} = k_0 + k_Q[\text{Q}] \quad (8)$$

Addition of sodium methoxide also resulted in efficient quenching of the absorptions due to the complexes, and the resulting plots of k_{decay} vs $[\text{Q}]$ were linear in the cases of **8a–d** (Figure 3b). Distinctly different behavior was observed upon addition of MeONa to the solutions of the *para*-trifluoromethylphenyl derivative (**1e**) in MeOH, where the transient absorptions (recorded at 330 nm) intensified and displayed a discernible growth component even at low methoxide ion concentrations. The transient lifetime decreased with increasing concentration up to ca. 1 mM in added MeONa and then leveled off to a value of $\tau \approx 300 \text{ ns}$ as the concentration was increased further. A lower limit of $k_Q \geq 3.7 \times 10^9 \text{ M}^{-1} \text{ s}^{-1}$ was estimated for the quenching rate constant from the k_{decay} value obtained in the presence of 0.26 mM MeONa, the lowest concentration that was studied in the experiment.

Transient spectra recorded for solutions of **1e** in MeOH in the absence and presence of 5.1 mM MeONa are shown in Figure 4 and clearly indicate that a new transient product is formed upon reaction of **8e** with methoxide ion. On the basis of the results of experiments carried out in THF in the presence of MeONa/MeOH (*vide infra*), we assign the species to germyl anion **10e** (eq 9).

Quenching of the **2e**–MeOD complex (**8e-d**) by MeSO_3H afforded a rate constant of $k_Q = (3.0 \pm 0.2) \times 10^8 \text{ M}^{-1} \text{ s}^{-1}$, leading to $k_{\text{H}}/k_{\text{D}} = 2.2 \pm 0.2$ and the conclusion that protonation at germanium occurs in the rate-determining step for reaction

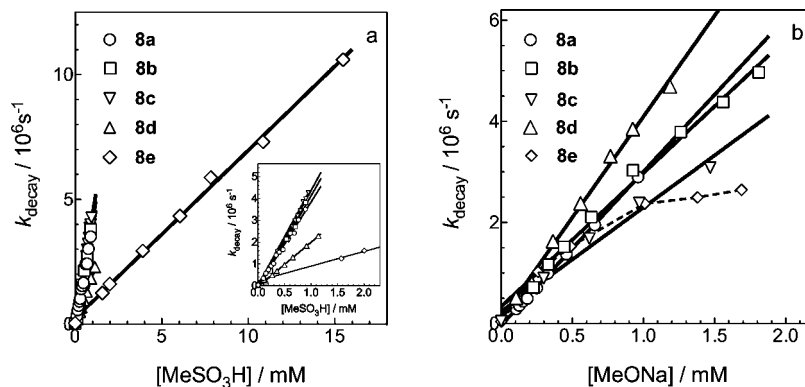


Figure 3. Plots of k_{decay} vs $[Q]$ for the quenching of $\text{GeAr}_2\text{-MeOH}$ complexes (**8a–e**) by (a) MeSO_3H and (b) MeONa in MeOH at 25°C . The inset in (a) shows an expansion of the plot over the 0–2.3 mM range in added acid. The solid lines are the linear least-squares fits of the data to eq 8.

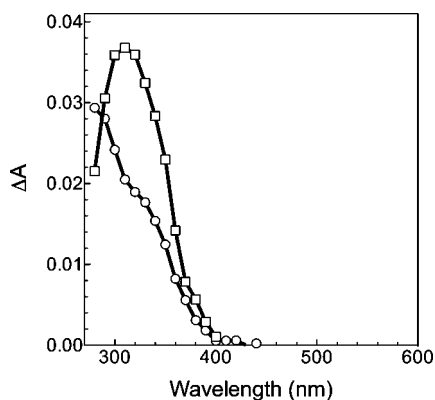
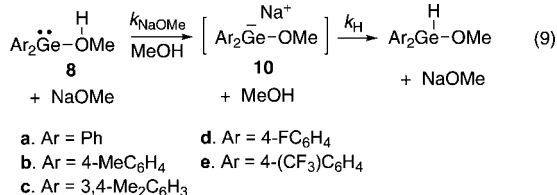
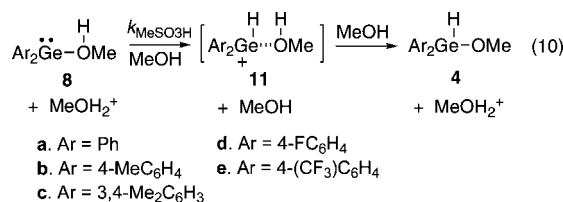


Figure 4. Transient absorption spectra from laser flash photolysis of **1e** in deoxygenated MeOH , recorded 0–0.64 μs after the pulse (–O–; $\tau \approx 25 \mu\text{s}$), and in MeOH containing 5.1 mM MeONa , 0.14–0.15 μs after the pulse (–□–; $\tau \approx 300 \text{ ns}$).



of the complex with acid. This is supported by the Hammett reaction constant of $\rho = -0.56 \pm 0.08$, obtained from a Hammett plot of the rate constants for quenching of **8a–e** by MeSO_3H (see Figure 5a), which is indicative of significant positive charge development at germanium in the transition state for the reaction. Equation 10 depicts the process in terms of the intermediacy of the corresponding germyl cations **11**, though we are unable to rule out a mechanism in which protonation occurs in concert with nucleophilic attack and a second proton transfer to the solvent. Interestingly, a transient spectrum recorded by laser photolysis of **1c** in MeOH containing 0.9 mM MeSO_3H appeared to be distinctly different than that in the absence of added acid, showing the long-wavelength absorption due to **8c** as a shoulder on a stronger absorption band centered at $\lambda_{\text{max}} \approx 290 \text{ nm}$ (Figure S7, Supporting Information). The decay kinetics were the same throughout the 280–360 nm monitoring range ($\tau \approx 210 \text{ ns}$), indicating that if the 290 nm absorption is due to a distinct species (such as cation **11c**), it is in mobile equilibrium with the complex. Unfortunately, the short time scale that was required for recording the spectrum, coupled with interference from fluorescence, makes it difficult to

ascertain with certainty whether the spectrum in acidic MeOH is really different from that recorded in the neutral solvent.



The trend in the rate constants for quenching of **8a–e** by methoxide ion is consistent with some degree of negative charge development at germanium in the rate-determining step of the reaction, though the correlation with Hammett substituent constants is poor ($\rho = +0.16 \pm 0.08$; see Figure 5b). Exclusion of **8e** from the analysis, which may be justified on the basis of the higher uncertainty in the k_{MeONa} value and the fact that its behavior is clearly different from the others, results in a much better correlation ($\rho = +0.45 \pm 0.11$; see dashed line in Figure 5b). Reaction of the **2a–MeOD** complex with MeONa was found to proceed with a rate constant of $k_{\text{Q}} = (2.13 \pm 0.06) \times 10^9 \text{ M}^{-1} \text{ s}^{-1}$, affording a solvent isotope effect of $k_{\text{H}}/k_{\text{D}} = 1.40 \pm 0.07$ for the parent diarylgermylene. It is unclear whether the isotope effect should be interpreted as a combination of primary and secondary effects resulting from rate-determining deprotonation of the complex by the added base or as a combination of purely secondary effects resulting from a nucleophilic substitution mechanism in which MeO^- displaces MeOL ($\text{L} = \text{H}$ or D) from the (monocoordinate)germylene–alcohol complex.

The $\text{GeMe}_2\text{-MeOH}$ complex (**9**) was also quenched efficiently by added MeSO_3H and MeONa . Plots of k_{decay} vs $[Q]$ showed excellent linearity over the 0–0.6 and 0–2.0 mM concentration ranges in acid and base, respectively, analysis of which afforded values of $k_{\text{MeSO}_3\text{H}} = (7.7 \pm 0.9) \times 10^9 \text{ M}^{-1} \text{ s}^{-1}$ and $k_{\text{MeONa}} = (1.8 \pm 0.2) \times 10^9 \text{ M}^{-1} \text{ s}^{-1}$ (Figure S8, Supporting Information). The greater reactivity of **9** toward MeSO_3H and lower reactivity toward MeONa compared to **8a** under the same conditions are consistent with inductive effects playing the dominant role in controlling the relative ion stabilities, since phenyl is weakly inductively electron-withdrawing relative to methyl.⁴⁷

Complex **9** was also quenched by added AcOH ($\text{p}K_{\text{a}} = 9.63$ in MeOH at 25°C ⁴⁸), and a plot of k_{decay} vs $[\text{AcOH}]$ was linear

(47) Hansch, C.; Leo, A.; Taft, R. W. *Chem. Rev.* **1991**, *91*, 165.

(48) Rived, F.; Roses, M.; Bosch, E. *Anal. Chim. Acta* **1998**, *374*, 309.

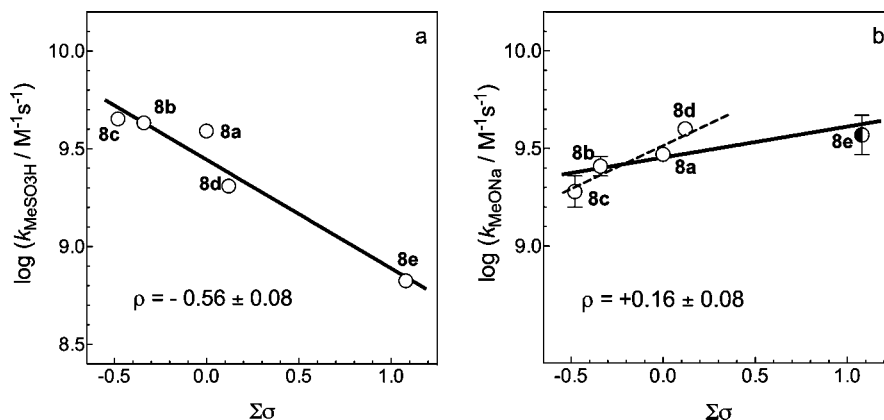
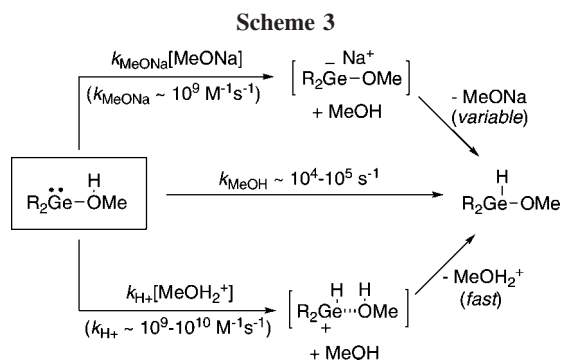


Figure 5. Hammett plots for the quenching of $\text{GeAr}_2\text{-MeOH}$ complexes (**8a–e**) by (a) MeSO_3H and (b) MeONa in MeOH solution at 25 °C. Hammett σ -values were taken from ref 47.

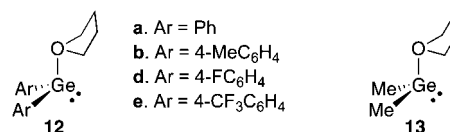


over the 0.001–0.15 M concentration range with slope $k_{\text{AcOH}} = (4.9 \pm 0.2) \times 10^7 \text{ M}^{-1} \text{ s}^{-1}$ (Figure S9, Supporting Information). The value is roughly 200 times lower than that for quenching by the much stronger acid, MeSO_3H . The $\text{p}K_{\text{a}}$ of MeSO_3H in MeOH has evidently not been reported, but an estimate of between 2 and 3 can be made on the basis of the aqueous $\text{p}K_{\text{a}}$ (−1.86 at 25 °C⁴⁹) and the difference of ca. +5 that is typical of the $\text{p}K_{\text{a}}$ values of carboxylic acids in methanol and water.⁴⁸ For a value of $\text{p}K_{\text{a}} \approx 3$, the percent dissociation of MeSO_3H ranges from ca. 54% to 22% over the 1–15 mM nominal concentration range in added acid, so a plot of k_{decay} vs the nominal MeSO_3H concentration should exhibit downward curvature if specific catalysis was responsible for the reaction of the gerylene– MeOH complexes in the presence of the added acid. Thus, the excellent linearity in the plots of k_{decay} vs $[\text{MeSO}_3\text{H}]$ for all six of the gerylene– MeOH complexes studied in this work is consistent with a general catalysis mechanism; the observed rate constant is then an average of contributions from catalysis by the lyonium ion (MeOH_2^+) and the general acid (MeSO_3H). The magnitude of these individual contributions must be quite similar to one another; indeed, the rate constant for quenching of **8a** by trifluoromethanesulfonic acid in MeOH was found to be $k_{\text{CF}_3\text{SO}_3\text{H}} = (3.1 \pm 0.3) \times 10^9 \text{ M}^{-1} \text{ s}^{-1}$ (Figure S10, Supporting Information), in good agreement with that for quenching by MeSO_3H under similar conditions.

Scheme 3 summarizes the kinetic behavior of the $\text{R}_2\text{Ge-MeOH}$ complexes studied in this work, in neat MeOH solution under neutral, basic, and acidic conditions.

Gerylene–THF Complexes in THF. Transient absorption spectra and representative decays from laser photolysis of

deoxygenated solutions of **1a** and **3** in THF are shown in Figure 6. The spectra of the **2**–THF complexes (**12**) are also blue-shifted relative to their positions in dilute hexane, but to a smaller degree ($\Delta\lambda_{\text{max}} \approx 15 \text{ nm}$) than that observed for the **2**– MeOH complexes ($\Delta\lambda_{\text{max}} \approx 30 \text{ nm}$; *vide supra*). A similar trend is evident in dilute hexane, though the effect is much more modest than in the neat liquids; for example, the absorption maximum of free **2a** ($\lambda_{\text{max}} = 500 \text{ nm}$ ⁴⁴) shifts to 355 and 350 nm in hexane containing millimolar concentrations of THF and MeOH , respectively.²⁴ It should be noted that the equilibrium constant for complexation of GePh_2 with THF in hexane is roughly an order of magnitude *larger* than that for complexation with MeOH under the same conditions,²⁴ and similar differences apply to GeMe_2 as well.²⁴ There is thus no correlation between the relative thermodynamic stabilities of the $\text{GeR}_2\text{-THF}$ and $\text{GeR}_2\text{-MeOH}$ complexes in dilute hexane solution and the relative magnitudes of the spectral shifts that result from complexation.



As in dilute hexane solution,²⁷ formation of the corresponding digermene and higher oligomers remains an important mode of decay of the gerylene–THF complexes in neat THF, though our ability to actually detect the digermene varied depending on the laser intensity and (presumably) the rigor with which the solvent was dried. For example, while the formation of Ge_2Me_4 ($\lambda_{\text{max}} = 370 \text{ nm}$ ^{44,45,50}) is clearly evident in the spectra of Figure 6b, we could find no indication of formation of the corresponding digermene dimer from GePh_2 (i.e., Ge_2Ph_4 ; $\lambda_{\text{max}} = 440 \text{ nm}$) in experiments with **1a** in THF (see Figure 6a, for example). We were only occasionally successful in detecting the formation of the tetraaryldigermenes in this solvent, though when we did the signals tended to be relatively weak and shorter-lived than in hexane. Nevertheless, the spectra of Figure 6a and 6b both show the characteristic *secondary* signs of digermene formation: long-lived transient absorptions ($\tau > 1 \text{ ms}$) that appear at the short-wavelength edge of our detection window, which we have assigned previously to higher gerylene oligomers.^{26,27,44,45} The strength of these signals and their substantial spectral overlap with those due to the complexes

(49) Serjeant, E. P.; Dempsey, B., *Ionisation of Organic Acids in Aqueous Solution*; Pergamon Press: New York, 1979; p 989.

(50) Mochida, K.; Kayamori, T.; Wakasa, M.; Hayashi, H.; Egorov, M. P. *Organometallics* **2000**, *19*, 3379.

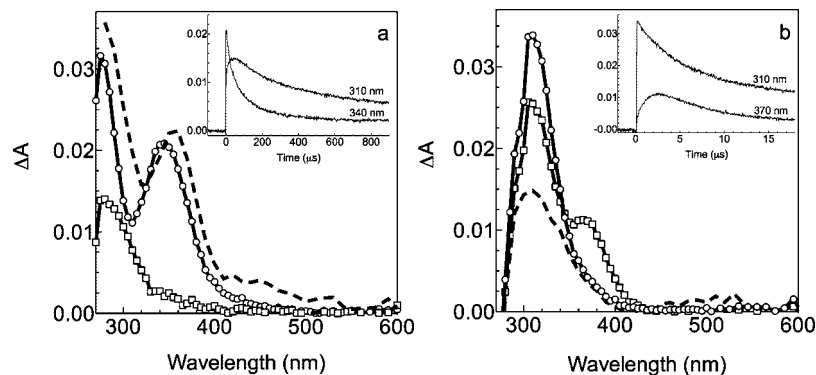


Figure 6. Transient absorption spectra from laser flash photolysis of **1a** and **3** in deoxygenated THF solution: (a) **1a**, recorded 0–3.2 μs (\circ) and 500–506 μs (\square) after the laser pulse (the inset shows transient decay traces recorded at 310 and 340 nm); (b) **3**, recorded 0.16–0.29 μs (\triangle) and 2.8–3.0 μs (\square) after the laser pulse (the inset shows transient decay traces recorded at 310 and 370 nm). The dashed lines show the spectra obtained from the same compounds in hexane containing (a) 2 mM and (b) 15 mM THF, recorded 0.1–0.2 μs after the pulse.

make it impossible to determine dimerization rate constants without resorting to spectral subtraction, which we have not undertaken. In contrast to the comparative ease with which Ge_2Me_4 can be detected from **3** in THF solution, our varied success in detecting the tetraaryldigermenes in laser photolysis experiments with **1a,b,d,e** under similar conditions (**1c** was not investigated) is most likely due to the combination of a lower rate of formation and greater rate of decay (due to reaction with residual water) in the ether solvent compared to that of Ge_2Me_4 . Interestingly, the formation of Ge_2Me_4 via dimerization of the GeMe_2 –THF complex appears to occur on a similar time scale in THF to that in pure hexane, where dimerization proceeds via the *free* germylene.⁴⁵ The difference in the dimerization kinetics of GeMe_2 and GePh_2 in THF relative to hexane likely results from steric effects on the rates being magnified significantly in the ether solvent relative to hexane. This is also true of subsequent steps in the oligomerization process, as evidenced by the fact that the time scale over which oligomerization of GePh_2 occurs is much longer in THF than in hexane and vastly exceeds that for the analogous process with GeMe_2 (see Figure 6). This effect is even more pronounced with the more highly hindered germylene GeMes_2 (*Mes* = mesityl), whose oligomerization stops with the formation of tetramesityldigermene (Ge_2Mes_4) in THF but proceeds further in noncomplexing solvents.^{24,51}

The reactivity of the GeMe_2 –THF complex (**13**) in THF toward a selection of representative substrates that we have characterized previously for the free germylene in hexane solution⁴⁵ was examined, including isoprene, 4,4-dimethyl-1-pentene (DMP), carbon tetrachloride (CCl_4), oxygen (O_2), and acetic acid (AcOH); in addition, quenching by MeSO_3H and MeONa/MeOH was also studied.

The results of these experiments are summarized in Table 2, along with the previously reported rate constants for reaction of the same substrates with free GeMe_2 in hexane.⁴⁵ Addition of up to 8 mM isoprene or 0.1 M DMP had no discernible effect on the decay characteristics of the complex, which establishes a (very liberal) estimate of $(2\text{--}4) \times 10^6 \text{ M}^{-1} \text{ s}^{-1}$ for the upper limit of the rate constants in these two cases. These can be compared to the reported values of $(1.1 \pm 0.3) \times 10^{10}$ and $(8.9 \pm 0.8) \times 10^9 \text{ M}^{-1} \text{ s}^{-1}$, respectively, for reaction of these two substrates with free GeMe_2 in hexane at 25 $^\circ\text{C}$.⁴⁵ The substantially lower reactivity of the germylene–THF complex toward

Table 2. Absolute Rate Constants (in units of $10^8 \text{ M}^{-1} \text{ s}^{-1}$) for Quenching of the GeMe_2 –THF Complex (**13**) in THF and Free GeMe_2 in Hexane⁴⁵ by Representative Substrates at 25 $^\circ\text{C}$ ^a

	GeMe_2 –THF complex in THF ($\lambda_{\text{max}} \leq 310 \text{ nm}$) $k_{\text{Q}}/10^8 \text{ M}^{-1} \text{ s}^{-1}$	GeMe_2 in hexane ($\lambda_{\text{max}} = 470 \text{ nm}$) ^b $k_{\text{Q}}/10^8 \text{ M}^{-1} \text{ s}^{-1}$
isoprene	$<0.04^c$	108 ± 28
DMP ^d	$<0.023^e$	89 ± 8
CCl_4	0.33 ± 0.03	0.8 ± 0.2
O_2	0.16 ± 0.05^f	0.9 ± 0.1
AcOH	0.14 ± 0.01	75 ± 4
MeSO_3H	0.73 ± 0.05	
MeONa/MeOH	11.4 ± 0.8	

^a Errors reported as $\pm 2\sigma$. ^b From ref 45. ^c Upper limit calculated from k_{decay} in the presence of 8 mM diene. ^d DMP = 4,4-dimethyl-1-pentene. ^e Upper limit calculated from k_{decay} in the presence of 0.1 M alkene. ^f Calculated from the first-order lifetime of the complex in O_2 -saturated THF.

these two substrates compared to that of the free germylene in hexane is consistent with the latter playing the role of the electrophile in the initial step of its reactions with aliphatic alkenes and dienes, as predicted by theory.^{41,52–54}

On the other hand, addition of CCl_4 led to discrete accelerations in the decay rate of the complex, and the resulting (linear) plot of k_{decay} vs $[\text{CCl}_4]$ afforded a rate constant of $k_{\text{CCl}_4} = (3.3 \pm 0.3) \times 10^7 \text{ M}^{-1} \text{ s}^{-1}$. This can be compared to the value of $8 \times 10^7 \text{ M}^{-1} \text{ s}^{-1}$ reported by us previously for the reaction of free GeMe_2 with CCl_4 in hexane.⁴⁵ In hydrocarbon solvents, the major products of the reaction are Me_2GeCl_2 and C_2Cl_6 , derived from initial Cl-atom abstraction to yield the chlorodimethylgermyl and trichloromethyl radicals as a singlet radical pair;^{55,56} we assume the reaction follows a similar course in THF, though this has not been specifically determined. The reactions of germynes with halocarbons are generally thought to proceed via the initial formation of a Lewis acid–base complex^{2,30,57} and are further known to exhibit a number of

(52) Sakai, S. *Int. J. Quantum Chem.* **1998**, *70*, 291.

(53) Su, M. D.; Chu, S. Y. *J. Am. Chem. Soc.* **1999**, *121*, 11478.

(54) Becerra, R.; Boganov, S. E.; Egorov, M. P.; Faustov, V. I.; Promyslov, V. M.; Nefedov, O. M.; Walsh, R. *Phys. Chem. Chem. Phys.* **2002**, *4*, 5079.

(55) Köcher, J.; Lehnig, M.; Neumann, W. P. *Organometallics* **1988**, *7*, 1201.

(56) Adachi, M.; Mochida, K.; Wakasa, M.; Hayashi, H. *Main Group Met. Chem.* **1999**, *22*, 227.

(57) Ohgaki, H.; Ando, W. *J. Organomet. Chem.* **1996**, *521*, 387.

(51) Hurni, K. L.; Rugar, P. A.; Payne, N. C.; Baines, K. M. *Organometallics* **2007**, *26*, 5569.

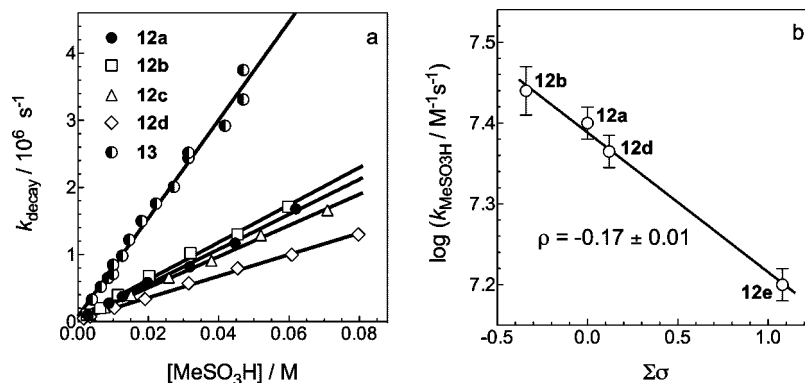


Figure 7. (a) Plots of k_{decay} vs $[Q]$ for the quenching of germylene–THF complexes by MeSO_3H in THF at 25 °C; the solid lines are the linear least-squares fits of the data to eq 8. (b) Hammett plot for the quenching of GeAr_2 –THF complexes (**12**) by MeSO_3H in THF solution at 25 °C.

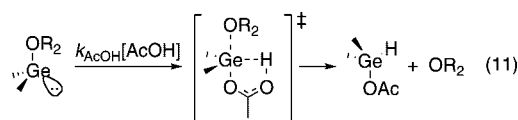
features characteristic of electron transfer reactions.^{26,58} If precomplexation with the halocarbon is a necessary component of the reaction in both THF and hydrocarbon solution, then a rate reduction is expected in THF, where the only kinetically significant species present is the germylene–solvent complex. On the other hand, electron transfer would be expected to be accelerated in the more polar solvent and, thus, might compensate for the rate reduction that is induced by the complexation pre-equilibria. A more detailed study of the effects of substituent and solvent on the reaction of germylenes with halocarbons is in progress in our laboratory, in an attempt to address these mechanistic issues more conclusively.

The decay of the complex was accelerated and proceeded with approximate pseudo-first order kinetics in O_2 -saturated THF, $k_{\text{decay}} = (1.59 \pm 0.02) \times 10^5 \text{ s}^{-1}$. This affords an estimated rate constant of $k_{\text{O}_2} \sim 1.6 \times 10^7 \text{ M}^{-1} \text{ s}^{-1}$ for quenching of the complex by molecular oxygen.

Quenching of the GeMe_2 –THF complex (**13**) by MeSO_3H proceeds with clean overall second-order kinetics (see Figure 7a) and a rate constant of $k_{\text{MeONa}} = (7.3 \pm 0.5) \times 10^7 \text{ M}^{-1} \text{ s}^{-1}$, roughly 100 times slower than the corresponding reaction of GeMe_2 –MeOH (**9**) in MeOH. The difference is ascribable to the much lower acidity of MeSO_3H in the aprotic solvent, for which a $\text{p}K_{\text{a}}$ on the order of ca. 15 can be estimated based on the value of $\text{p}K_{\text{a}} \approx 7.8$ reported for $\text{CF}_3\text{SO}_3\text{H}$ in THF.⁵⁹ Similar results were obtained for quenching of the GeAr_2 –THF complexes by MeSO_3H (see Figure 7a). The rate constants varied only modestly with substituent, but the resulting Hammett plot showed excellent linearity (see Figure 7b) and afforded a reaction constant of $\rho = -0.17 \pm 0.01$, indicative of only slight positive charge development at germanium in the rate-determining step for reaction. Thus, acid quenching by MeSO_3H in THF involves a transition state in which positive charge at Ge is significantly less well-developed than is the case in MeOH solution, where the acid strength is much higher and the rate constants are more than 2 orders of magnitude larger.

Quenching of **13** by AcOH ($\text{p}K_{\text{a}} = 24.4$ in THF⁶⁰) proceeds with a rate constant of $k_{\text{AcOH}} = (1.3 \pm 0.1) \times 10^7 \text{ M}^{-1} \text{ s}^{-1}$, only ca. 5 times slower than quenching by MeSO_3H . The rate constant was found to exhibit a primary kinetic deuterium isotope effect of $k_{\text{H}}/k_{\text{D}} = 2.8 \pm 0.4$ (Figure S11, Supporting

Information), consistent with significant O–H(D) bond rupture in the transition state for the rate-determining step of the reaction. Taken together, the results for both MeSO_3H and AcOH are most consistent with a mechanism involving concerted displacement of solvent and proton transfer from the substrate to germanium in the complex, as illustrated in eq 11 for the reaction of GeMe_2 –THF with AcOH. As might be expected, addition of up to 0.5 M MeOH had no detectable effect on the decay characteristics of the GeMe_2 –THF complex.



In contrast to the patterns of reactivity described above, reaction of **13** with MeONa (added as a 0.1 M solution in MeOH) proceeds rapidly. A rate constant of $k_{\text{MeONa}} = (1.14 \pm 0.08) \times 10^9 \text{ M}^{-1} \text{ s}^{-1}$ was obtained from a (linear) plot of k_{decay} vs methoxide concentration, only ca. 35% lower than that for reaction of the same substrate with the GeMe_2 –MeOH complex (**9**) in MeOH. The similarity in the rate constants suggests that the two reactions may proceed via a common nucleophilic displacement mechanism, the only one possible for the germylene–ether complex. The primary product of the reaction is presumed to be the $\text{Me}_2(\text{MeO})\text{Ge}^-$ anion, though no evidence for the formation of a new transient species that might be assigned to the anion was obtained in the experiment.

Considerably different results were obtained for the GeAr_2 –THF complexes (**12**), for which addition of small amounts of MeONa as a 0.5 M solution in MeOH caused the transient profiles to take on a bimodal form consisting of a rapid growth and subsequent decay, consistent with the formation of a new transient product. For example, Figure 8 shows transient spectra and representative transient absorption–time profiles, recorded by laser photolysis of a deoxygenated solution of **1a** in THF containing 7.5 mM MeONa/0.37 M MeOH. The spectrum of the new transient product is quite similar to that reported by Mochida and co-workers for (methyl)diphenylgermyl)lithium ($\text{Ph}_2\text{MeGe}^-\text{Li}^+$) in THF solution ($\lambda_{\text{max}} = 310 \text{ nm}$)⁶¹ and is thus assigned to the $\text{Ph}_2(\text{MeO})\text{Ge}^-$ anion (**10a**). The absorption grows in over the first 2 μs after excitation and then decays with clean pseudo-first-order kinetics and lifetime $\tau \approx 7 \mu\text{s}$. The growth of the signal occurs over the same time scale

(58) Egorov, M. P.; Gal'minas, A. M.; Basova, A. A.; Nefedov, O. M. *Dokl. Akad. Nauk. SSSR (Engl. transl.)* **1993**, 329, 102.

(59) Deshmukh, B. K.; Siddiqui, S.; Coetzee, J. F. *J. Electrochem. Soc.* **1991**, 138, 124.

(60) Barron, D.; Buti, S.; Ruiz, M.; Barbosa, J. *Phys. Chem. Chem. Phys.* **1999**, 1, 295.

(61) Mochida, K.; Wakasa, M.; Sakaguchi, Y.; Hayashi, H. *J. Am. Chem. Soc.* **1987**, 109, 7942.

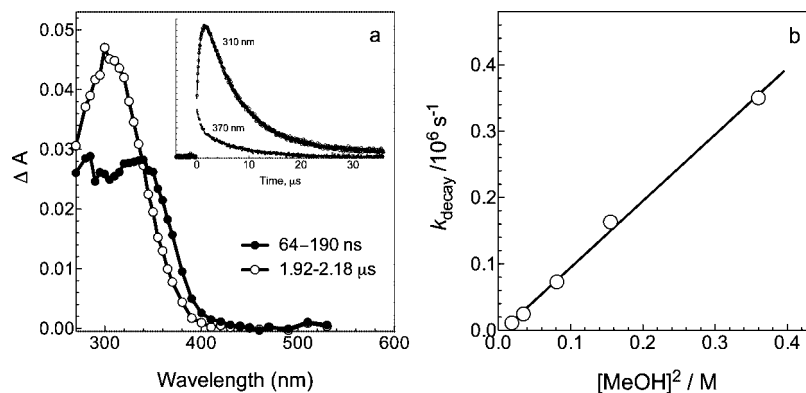


Figure 8. (a) Transient absorption spectra from laser flash photolysis of **1a** in deoxygenated THF containing 7.5 mM MeONa + 0.4 M MeOH, recorded 64–190 ns (●) and 1.9–2.2 μs (○) after the laser pulse; the inset shows two of the transient absorption–time profiles from which the spectra were derived, recorded at 310 and 370 nm. (b) Plot of k_{decay} vs $[\text{MeOH}]^2$ for quenching of anion **10a** ($\lambda_{\text{max}} = 310$ nm) by MeOH at 25 °C.

as the early portion of the bimodal decay of the signals at longer wavelengths, which are dominated by absorptions due to the germylene–solvent complex, and can thus be assigned to the formation of anion **10a** due to reaction of **12a** with methoxide ion. Fitting of the 310 nm growth–decay profile to the sum of two first-order exponentials afforded rate coefficients of $k_{\text{growth}} = (1.40 \pm 0.02) \times 10^6 \text{ s}^{-1}$ and $k_{\text{decay}} = (1.46 \pm 0.01) \times 10^5 \text{ s}^{-1}$ for the growth and decay components, respectively; the latter was accelerated upon addition of pure MeOH to the solution, consistent with protonation being the process responsible for the decay. Both components of the growth–decay profile responded in a nonlinear fashion to changes in the substrate concentrations, for reasons that we do not yet fully understand. While a plot of k_{decay} vs $[\text{MeOH}]^2$ was linear and afforded a third-order rate coefficient of $k = (1.00 \pm 0.07) \times 10^6 \text{ M}^{-2} \text{ s}^{-1}$ (see Figure 8b), the analogous plot of the growth rate constants (i.e., k_{growth} vs $[\text{MeONa}]^2$) remained nonlinear. The latter is probably at least partly due to the near coincidence of the spectra of the complex and the anion, which causes the growth component of the anion signal to contain opposing contributions from both species.

Analogous results were obtained with solutions of **1b**, **1d**, and **1e** in THF (Figure S12, Supporting Information) containing 8–8.5 mM MeONa and ca. 0.4 M MeOH. The UV spectra of the corresponding anions vary irregularly as a function of substituent; for example, while those of **10a** and **10e** exhibit well-defined absorption bands with maxima at 310 and 335 nm, respectively, the spectra of **10b** and **10d** have more the appearance of edge absorptions, with apparent maxima at 295 and 285 nm, respectively. On the other hand, the growth and decay rate constants of the species both followed regular trends with substituent, those for the growth increasing over roughly an order of magnitude with increasing electron-withdrawing power of the aryl substituents, and those for the decay decreasing correspondingly. As with **10a**, plots of k_{decay} vs $[\text{MeOH}]^2$ for the three substituted derivatives were approximately linear, affording values of $k_{2\text{MeOH}}$ ranging from ca. $1 \times 10^4 \text{ M}^{-2} \text{ s}^{-1}$ for **10e** to ca. $2.5 \times 10^6 \text{ M}^{-2} \text{ s}^{-1}$ for **10b**. The value of $k_{2\text{MeOH}}$ determined for **10e** yields an extrapolated lifetime of $\tau \approx 170$ ns for this derivative in neat MeOH solution, in reasonable agreement with the experimentally measured lifetime under these conditions (*vide supra*). A plot of $\log(k_{2\text{MeOH}}/\text{M}^{-2} \text{ s}^{-1})$ vs Hammett substituent constants was linear and afforded a slope of $\rho = -1.80 \pm 0.13$ (Figure S13, Supporting Information). The effect of substituents on the rate of formation of the anion was approximated using growth rate constants recorded at the

Table 3. Spectroscopic and Kinetic Data for GeAr₂–THF Complexes (12**) and the Corresponding Ar₂(MeO)Ge[−] Anions (**10**) in THF Solution at 25 °C^a**

4-X ^b	GeAr ₂ –THF (12)			Ar ₂ (MeO)Ge [−] (10)		
	λ_{max} (nm)	$k_{\text{MeSO}_3\text{H}}/10^7 \text{ M}^{-1} \text{ s}^{-1}$	$k_{\text{MeONa}}/10^8 \text{ M}^{-1} \text{ s}^{-1}$	λ_{max} (nm)	τ^d (μs)	$k_{2\text{MeOH}}/10^6 \text{ M}^{-2} \text{ s}^{-1}$
H (a)	345	2.60 ± 0.12	1.8 ± 0.6	310	6.8	1.00 ± 0.07
CH ₃ (b)	340	2.79 ± 0.08	3.4 ± 1.2	295	2.0	2.5 ± 0.1
F (d)	335	2.32 ± 0.04	6.5 ± 0.5	285	18	0.35 ± 0.04
CF ₃ (e)	335 (sh)	1.61 ± 0.03	25 ± 1	335	280	0.0097 ± 0.0009

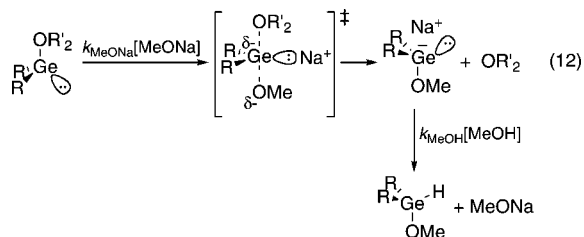
^a Errors reported as $\pm 2\sigma$. ^b Ring substituent in Ar. ^c Estimated from the rate coefficient for growth of the anion absorption in the presence of 7.5–8.5 mM NaOMe, determined by nonlinear least-squares fitting of the anion growth–decay profiles to the sum of two exponentials ($k_{\text{MeONa}} \equiv k_{\text{growth}}/[\text{MeONa}]$). ^d First-order lifetime of the anion absorption in the presence of ca. 0.4 M MeOH. ^e From (linear) plots of k_{decay} vs $[\text{MeOH}]^2$.

highest methoxide concentrations studied (7.5–8.5 mM), corrected for the concentration. The resulting Hammett plot showed acceptable linearity and afforded a ρ -value of $+0.70 \pm 0.25$.

Table 3 lists the UV-absorption maxima of the Ar₂Ge–THF complexes (**12**) and corresponding Ar₂(MeO)Ge[−] anions (**10**), along with the rate coefficients for quenching of the complexes by MeSO₃H and MeONa, and the anions by MeOH, in THF solution at 25 °C.

The estimated Hammett ρ -value for formation of the anions reflects the degree of negative charge development at germanium in the transition state for the reaction, which must proceed by nucleophilic substitution of the neutral THF moiety in the GeAr₂–THF complexes by methoxide ion (eq 12). Relatively few kinetic data have been reported for the formation or reactions of germyl anions; to our knowledge, the only relevant data that exist are those of Eaborn and Singh for the methoxide-catalyzed tritium–hydrogen exchange of triarylgermanes in MeOH, for which the rate-determining step is formation of the corresponding triarylgermyl anions by tritium transfer.⁶² The absolute rate constants are many orders of magnitude lower than those reported here for the reactions of methoxide ion with **12** (e.g., $k = 1.4 \times 10^{-3} \text{ M}^{-1} \text{ s}^{-1}$ for detritiation of Ph₃GeT at 20 °C⁶²), and the Hammett ρ -value ($= +2.2$ ⁶²) is considerably more positive. Interestingly however, the latter is similar in magnitude to that characterizing the protonation of **10** by MeOH in THF. To the extent that a direct comparison can be justified, this supports the conclusion of the earlier workers that protonation involves a transition state in which the proton is roughly half-transferred from the alcohol to germanium.⁶²

(62) Eaborn, C.; Singh, B. J. *Organomet. Chem.* **1979**, *177*, 333.



It is important to recognize that despite the substantial exergonicity associated with the conversion of the GeR_2 –THF complexes to the corresponding methoxygermanes via reaction with MeONa/MeOH , which is implied by the rapidity of the individual steps in the two-step sequence, the process is characterized by a mobile reversibility. This is evident from the early work of Satgé and co-workers on the chemistry of alkoxyhydridogermanes such as $\text{Me}_2\text{Ge}(\text{H})\text{OMe}$ and **4a**, which showed these compounds to be readily transformed into the products of germylene oligomerization under basic conditions.⁶³

Summary and Conclusions

The Lewis acid–base complexes of GeMe_2 , GePh_2 , and a series of ring-substituted diarylgermylenes with THF and MeOH can be easily detected in the neat O-donor solvents, as relatively long-lived transients exhibiting UV–vis absorption spectra that are blue-shifted significantly relative to their positions in dilute hexane solution. Dimerization, the normal fate of free germynes in the absence of reactive substrates, is generally slowed dramatically in THF compared to the situation in hexane solution. It appears to be eliminated in MeOH owing to solvent-catalyzed transfer of the OH proton in the complex to germanium, which yields the corresponding methoxyhydridogermane. This process is ca. 10 times faster for the GeMe_2 –MeOH complex than for the arylated systems, for which the rate constants show no consistent variation with ring substituent. It is thus concluded that the process most likely proceeds concertedly, and the slower rates that are observed for the arylated systems are due mainly to steric factors.

Reaction of the germylene–methanol complexes is accelerated quite significantly in the presence of added acids or base. The bimolecular rate constants for reaction of the GeMe_2 –MeOH complex with MeSO_3H and AcOH show a pronounced dependence on acid strength, with that for MeSO_3H approaching the diffusion limit. Solvent kinetic isotope and substituent effects on the rate constants for quenching of the GeAr_2 –MeOH complexes by MeSO_3H are consistent with significant positive charge development at germanium in the transition state for the reaction; however, if discrete cations are formed, they are trapped by the solvent too rapidly to be detected on the time scale of our experiments. Quenching by methoxide ion is equally rapid in the case of the GePh_2 –MeOH complex, but exhibits a small (normal) solvent isotope effect and only very modest increases in rate constant with increasing electron-withdrawing power of the ring substituents throughout the series studied. This makes it difficult to ascertain whether the reaction proceeds via deprotonation at oxygen or by a nucleophilic substitution mechanism in which neutral methanol is displaced from the complex by methoxide ion. Nevertheless, the reaction is thought to proceed via the initial formation of the corresponding methoxygermyl anion, which has been detected in one instance. In general however, these species are too short-lived

in MeOH solution to be detected as discrete intermediates. The data obtained in these experiments effectively characterize the reverse of the base-catalyzed α -elimination reaction of alkoxyhydridogermanes, which has been known for many years.⁶³

Reaction of the germylene–THF complexes with methoxide ion is also rapid and leads to the corresponding methoxygermyl anions, which are readily detectable in the cases of the diaryl systems. Their formation rates and lifetimes, of which the latter are limited by protonation by MeOH, increase dramatically with increasing electron-withdrawing power of the aryl ring substituents. The GeMe_2 –THF complex exhibits vastly reduced reactivities toward less potent nucleophiles such as aliphatic alkenes and dienes and MeOH, substrates that react with the free germylene at close to the diffusion-controlled rate in hexane solution. If anything, the complex is moderately nucleophilic, as indicated by its reactivity toward (weakly) acidic substrates such as acetic and methanesulfonic acid. Interestingly, of the reactions that have been studied so far, the only ones that appear to proceed at similar rates in THF and hexane solution are the those with O_2 and CCl_4 . The mechanistic details of these and other reactions of transient germynes in complexing and noncomplexing solvents are the subject of continued study in our laboratory.

Experimental Section

The germacyclopent-3-enes **1a,b,d,e** and **3** were synthesized and purified according to previously reported procedures;^{27,44,45} the synthesis, characterization, and basic photochemical behavior of **1c** are described in the Supporting Information. Methanol for laser flash photolysis experiments was HPLC grade and was used as received from Caledon Laboratories Ltd. Tetrahydrofuran (Caledon reagent) was dried by passage through activated neutral alumina (250 mesh; Aldrich) under nitrogen using a Solv-Tek solvent purification system. Methanesulfonic acid (Sigma-Aldrich) was distilled. Standard solutions of sodium methoxide were prepared from sodium metal and anhydrous methanol. CCl_4 was refluxed over phosphorus pentoxide and distilled. Isoprene and 4,4-dimethyl-1-pentene (DMP) were obtained from Sigma-Aldrich and were purified by passage of the neat liquids through a silica gel microcolumn. Glacial acetic acid, acetic acid-*O-d*, methanol-*O-d*, and trifluoromethanesulfonic acid were used as received from Sigma-Aldrich.

Nanosecond laser flash photolysis experiments were carried out using the pulses from a Lambda-Physik Compex 120 excimer laser, filled with $\text{F}_2/\text{Kr}/\text{Ne}$ (248 nm; ca. 20 ns; 100 ± 5 mJ), and a Luzchem Research mLFP-111 laser flash photolysis system, modified as described previously.⁴⁴ Solutions were prepared in a calibrated 100 mL reservoir, fitted with a glass frit to allow bubbling of argon, air, or oxygen through the solution for at least 30 min prior to and then throughout the duration of each experiment. Concentrations were such that the absorbance at the excitation wavelength was between ca. 0.7 and 0.9. The solutions were pumped from the reservoir through Teflon tubing (Cole-Parmer Instrument Co.) to a 7×7 mm Suprasil flow cell using a Masterflex 77390 peristaltic pump. The glassware, sample cell, and transfer lines were dried in a vacuum oven (65–85 °C) before use. Solution temperatures were measured with a Teflon-coated copper/constantan thermocouple inserted into the thermostated sample compartment in close proximity to the sample cell. Reagents were added directly to

the reservoir by microliter syringe as aliquots of standard solutions. Transient decay and growth rate constants were calculated by nonlinear least-squares analysis of the absorbance–time profiles using the Prism 5.0 software package (GraphPad Software, Inc.) and the appropriate user-defined fitting equations, after importing the raw data from the Luzchem mLFP software. Rate constants

(63) Massol, M.; Satgé, J.; Rivière, P.; Barrau, J. J. *Organomet. Chem.* **1970**, *22*, 599.

were calculated by linear least-squares analysis of decay rate–concentration data (generally 4–7 points) that spanned as large a range in transient decay rate as possible. Errors are quoted as twice the standard error obtained from the least-squares analyses.

Acknowledgment. We thank the Natural Sciences and Engineering Research Council of Canada for financial support, including scholarships to L.A.H. and S.S.C.

Supporting Information Available: Details of the synthesis and characterization of compounds and of steady state photolysis experiments; representative transient decay profiles; time-resolved UV/vis absorption spectra; plots of k_{decay} vs [Q] for the various systems studied. This material is available free of charge via the Internet at <http://pubs.acs.org>.

OM8010323